THE JOURNAL OF PHYSICAL CHEMISTRY B

Article

pubs.acs.org/JPCB

# Modeling of the Structure of Sodium Borosilicate Glasses Using Pair Potentials

Hiroyuki Inoue, Atsunobu Masuno,* and Yasuhiro Watanabe

Institute of Industrial Science, The University of Tokyo, 4-6-1 Komaba, Meguro-ku, Tokyo, 153-8505, Japan

**ABSTRACT:** Structural models of sodium borosilicate glasses were prepared by means of molecular dynamics (MD) technique using pair potentials over a wide compositional range. The local structures around B, O, and Si obtained from the structural models were compared with experimental $^{11}$B NMR, $^{17}$O NMR, and $^{29}$Si NMR data. It was found that atomic arrangements of B, O, and Si in the structural models were similar to the experimental results indicating that the simulations can reproduce the chemical bonds of the real glasses. These results confirm that even if the MD technique using the pair potentials is quite simple, it is enough to capture the essence of the amorphous materials. In the linkage of the cation−oxygen polyhedra, the differences were observed between the structural models and the experimental results. The factors responsible for these differences are discussed with respect to the equilibrium reactions between the cation−oxygen polyhedra at a higher temperature. The discussion suggests that the differences were caused by the extremely higher quenching rate than the real glasses as well as by the simplicity of our pair potential and the smaller size of the unit cell.

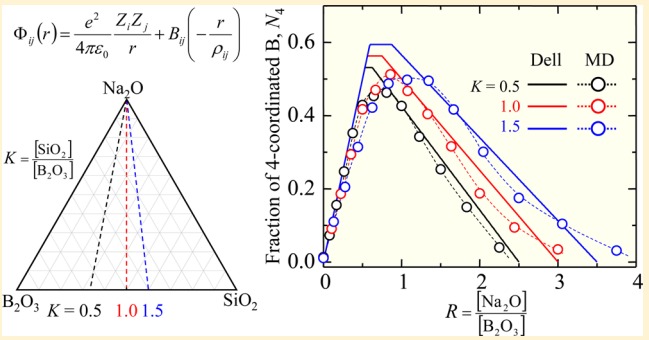


## I. INTRODUCTION

Borosilicate glasses are used in many applications such as a BK7 optical glass, Vycor porous glass, and N-51 A glass test tube. There have been a considerable number of reports about the atomic arrangement of borosilicate glasses in order to clarify the origin of their functionality.[1−11] In the case of sodium borosilicate glasses where the Na ions act as modifiers, the network consists of structural units such as $SiO_4$ and $BO_4$ tetrahedra and $BO_3$ triangles. A comprehensive structural model of the sodium borosilicate glasses, which described the relation among these structural units, was proposed in 1983 by Dell et al.[1] on the basis of experimental $^{11}$B NMR data. In Dell's model, at low sodium oxide content, each Na atom modifies the coordination number of a B atom from 3 to 4, and diborate groups ($Na_2O{\cdot}2B_2O_3$), which contain two $BO_4$ and two $BO_3$ units, are formed. The additional sodium oxide converts the diborate groups into reedmergnerite groups ($Na_2O{\cdot}B_2O_3{\cdot}8SiO_2$), which contain two $BO_4$ and eight $SiO_4$ units. Further addition of sodium oxide forms nonbridging oxygen (NBO) atoms at $SiO_4$ units in the reedmergnerite groups. At higher sodium oxide content, the diborate and reedmergnerite groups are destroyed. In Dell's model, the ratios $R = [Na_2O]/[B_2O_3]$ and $K = [SiO_2]/[B_2O_3]$ are important parameters. The variations in the structural units are organized according to the $K$ and $R$ values. Taking into account more recent experimental results, the revision of Dell's model has been proposed that alkali ions are more randomly distributed between silica and borate structure units.[11]

While the investigation of structural models progressed employing experimental data, a simulation of the structure of sodium borosilicate glasses was performed by Soules and Varshneya in 1981[12] using molecular dynamics (MD) and pair potentials. The four-coordinated B atoms and the effect of increasing the $K$ ratio could be reproduced in his report. Recently, Kieu et al.[13] have reported the simulation of sodium borosilicate glasses by using empirical potentials which is dependent on the glass chemical composition. They showed the reproducibility of the glass structure and mechanical properties as well as the structure of reedmergnite crystal. However, a systematic simulation of sodium borosilicate glasses with various glass compositions does not exist to date.

Recently, analytical methods such as $^{17}$O 3QMAS NMR,[3−5] $^{29}$Si magic angle spinning (MAS) NMR,[8,9] and X-ray photoelectron spectroscopy (XPS)[10] have improved. Accordingly, the quantity and quality of the obtained structural information has improved remarkably. Theoretical approaches and computing power have also developed to a great extent. Thus, it is time to prepare the atomic arrangement and local structure using high precision experimental results and computer simulations. In this study, structural models of sodium borosilicate glasses are prepared by means of MD using pair potentials over a wide composition. The structural models obtained by the MD simulation are compared with Dell's model as the results of $^{11}$B NMR experiment. Then, our structural models are compared with the resent results of $^{17}$O 3QMAS NMR and $^{29}$Si MAS NMR experiments.

**Received:** April 20, 2012
**Revised:** September 10, 2012
**Published:** September 10, 2012





dx.doi.org/10.1021/jp3038126 | J. Phys. Chem. B 2012, 116, 12325−12331

## II. CALCULATION METHODS

First, we simulate the crystalline $NaBO_2$ structure and obtain the set of optimal parameters for the B−O and Na−O pairs. Then, the parameters are accordingly modified to reproduce the fraction of $BO_4$ units in the experimental results for $Na_2O-B_2O_3$ glasses. Furthermore, we produced structural models of $Na_2O-B_2O_3-SiO_2$ glasses by using these parameters.

The Born-Mayer type of pair potentials used are given by

$$\Phi_{ij}(r_{ij}) = \frac{e^2}{4\pi\varepsilon_0}\frac{Z_iZ_j}{r_{ij}} + B_{ij}\exp\left(-\frac{r_{ij}}{\rho_{ij}}\right) \quad (1)$$

where $\Phi_{ij}$ is the interaction energy of the $i$ and $j$ ions, which consists of Coulomb and short-range repulsion terms, $e$ is the electron charge, $\varepsilon_0$ is the vacuum permittivity, $Z_i$ is the effective charge of the $i$ ion, $r_{ij}$ is the interatomic distance, $B_{ij}$ is an empirical constant, and $\rho_{ij}$ is the softness parameter. The value of $B_{ij}$ is obtained from the distance between $i$ and $j$ ions reaching a minimum at $R_{ij}$ using the following equation.

$$B_{ij} = -\frac{e^2}{4\pi\varepsilon_0}\frac{Z_iZ_j}{R_{ij}^2}\rho_{ij}\exp\left(\frac{R_{ij}}{\rho_{ij}}\right) \quad (2)$$

We set the parameters for $Z$, $B$, and $\rho$ for each atomic pair. For each cation−cation pair, the value of $B$ was fixed at zero. The effective charges of B, $Z_B$, and Na, $Z_{Na}$, were fixed at +1.8 and +1.0, respectively; the parameters of the O−O pair were also fixed. The Coulomb force was evaluated using the Ewald summation. The classical equations of motion were integrated using Verlet's algorithm. All simulations were carried out at constant volume at a time step of 1 fs. The MD code for the simulations was developed by us.

For simulating the $NaBO_2$ crystal structure, configurations containing 864 particles were initially located at ideal crystal coordinates.[14] Then, the structural simulations were carried out at 293 K with 20 000 time steps for several potential parameter sets. For structural models obtained with these parameters, the square displacement of each ion was estimated from the initial and final coordinates. The parameter sets were evaluated by the summation of the square displacement. Among the sets of parameters, the optimal set was established on the basis of the best reproducibility of the experimental frequencies of the Raman spectra. Raman spectra were simulated by taking into account correlated atomic vibrations in the B−O network. The Raman cross sections can be computed in the following form of the power spectra.[15]

$$I_{iso} = \frac{1}{2\pi}\left[\lim_{\tau\to\infty}\frac{1}{2\tau}\left|\int_{-\tau}^{\tau} dt e^{-i\omega t}\mathbf{P}_{iso}(t)\right|^2\right] \quad (3)$$

$$I_{aniso} = \frac{1}{2\pi}\sum_{i,j}\left[\lim_{\tau\to\infty}\frac{1}{2\tau}\left|\int_{-\tau}^{\tau} dt e^{-i\omega t}[\mathbf{P}_{aniso}]_{ij}(t)\right|^2\right] \quad (4)$$

The space-fixed Cartesian polarizability tensor $\mathbf{P}$ can be represented as the 3 × 3 matrix $\mathbf{P}_{ij}$, where $i$ and $j$ are each of the space-fixed axes $x$, $y$, or $z$. $\mathbf{P}_{iso}$ and $\mathbf{P}_{aniso}$ are the isotropic and anitotropic part of the polarizability tensor. For the B−O pair, of which distance was less than 2.0 Å, the polarizability was assumed to be in proportion to the distance of B−O pairs. Only the polarizability component along the B−O direction was assumed to be not zero.

Structural models of $Na_2O-B_2O_3$ glasses were prepared at 5% increments from 0% to 50% $Na_2O$ content by using the optimal parameter set obtained from the $NaBO_2$ crystal. The densities of the models were based on the experimental densities.[16] In the basic cell, there are 1000 cations and oxygen ions which counterbalance the cations. The charge of the oxygen ions was set on the basis of charge neutrality in the basic cell. Simulations were performed for random initial coordinates for each chemical composition. After 20 000 time steps at 4000 K, the temperature of the simulation was decreased from 4000 to 293 K at time steps of $10^5$. Then, the models were annealed at 293 K for 20 000 time steps. The parameters of the pair potentials were modified to reproduce the experimental data for the fraction of the four-coordinated B atoms in the $Na_2O-B_2O_3$ system.

Structural models of $Na_2O-B_2O_3-SiO_2$ glasses were prepared with 5% increments of $Na_2O$ from 0% to 60% at $K$ = 0.5, 1, 1.5, 2, 3, 4, and 6 by using the optimized potential parameters for the B−O and Na−O pairs in the $Na_2O-B_2O_3$ system. The potential parameters of the Si−O and O−O pairs adopted in a prior study[17] were also used. The densities of the models were the experimental densities.[16] In the basic cell, there were about 3000 ions. Simulation procedures were the same as in the $Na_2O-B_2O_3$ glasses.

## III. RESULTS

**(1). $NaBO_2$ Crystal.** Some sets of the parameters could maintain the crystal structure. They were evaluated by the summation of the square displacement of each ion from the initial and final coordinates. When the effective charge of B atoms was fixed at +1.8, the summation of the square displacement tended to decrease as the effective charge of Na atoms approached +1. Furthermore, the summation tended to show the minima at 2.03−2.08 Å in $R_{Na-O}$ and at 0.28−0.30 Å in $\rho_{Na-O}$. There are two kinds of the B−O pairs in the initial crystal structure of which distances are at 1.280 and 1.433 Å. After the simulation using one of the optimal parameter sets $R_{Na-O}$ = 2.08 Å, $R_{B-O}$ = 1.17 Å, $\rho_{Na-O}$ = 0.30 Å, and $\rho_{B-O}$ = 0.17 Å, the distances changed to around 1.30 and 1.37 Å and the distributions broadened. Slight changes were observed in the atomic arrangement and in its symmetry.

$I_{iso}$ spectrum, calculated for the structural model obtained by using this parameter set, is shown in Figure 1. According to Chryssikos et al., the six-membered metaborate ring $(BO_2O^-)_3$ shows $D_{3h}$ symmetry in $NaBO_2$ crystal.[18] Ten normal modes of

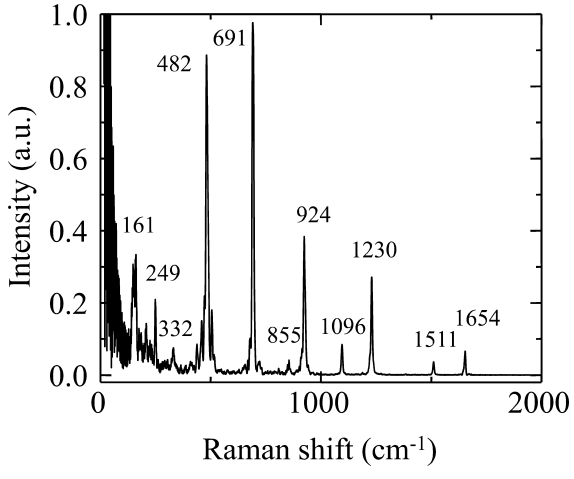


**Figure 1.** Calculated $I_{iso}$ spectrum of the simulated $NaBO_2$ crystal.


dx.doi.org/10.1021/jp3038126 | J. Phys. Chem. B 2012, 116, 12325−12331

21 normal modes are Raman active 2E″ + 5E′ + 3A$_1$′. For the experimental Raman spectra of $NaBO_2$ crystal, bands at 1575, 1554, 770, and 627 cm$^{-1}$ are assigned to A$_1$′ modes. The observed splitting into 1575 and 1554 cm$^{-1}$ is attributed to the boron isotope effect. A band at 682 cm$^{-1}$ is assigned to E″ mode, and bands at 475 and 399 cm$^{-1}$ are assigned to E′ modes.[18] The calculated $I_{iso}$ spectrum is composed of all Raman active modes, and $I_{aniso}$ spectrum is composed of modes E′ and E″. For the assignment of the calculated spectra, the assignment of the normal modes of the $CsBO_2$ crystal,[19] in which there is the same $D_{3h}$ ring, was referenced. A peak at 1654 cm$^{-1}$ in the $I_{iso}$ spectrum was assigned to the A$_1$′ mode of the B−O$^-$ stretching vibration. This peak seems to correspond to the experimental bands at 1575 and 1554 cm$^{-1}$. Peaks at 924 and 691 cm$^{-1}$ in the $I_{iso}$ spectrum were assigned to A$_1$′ modes of ring-breathing vibrations corresponding to the bands at 770 and 627 cm$^{-1}$ in the experimental spectrum. Among peaks at 1511, 1230, 1096, 482, and 332 cm$^{-1}$ assigned to E′ modes, the peaks at 482 and 332 cm$^{-1}$ correspond to the experimental bands at 475 and 399 cm$^{-1}$. Peaks at 855 and 161 cm$^{-1}$ may be assigned to the E″ modes of which the wavenumber is located at 682 cm$^{-1}$. Accordingly, in the simulation using simple two-body potentials, there were 20% differences in the wavenumbers at a maximum. It was shown that our simulations could reproduce the $NaBO_2$ crystal structure and vibration spectrum. These confirmed that the parameters used in the MD simulations were appropriate.

**(2). $Na_2O-B_2O_3$ Glasses.** We prepared structural models of $Na_2O-B_2O_3$ using the set of the parameters obtained from the $NaBO_2$ crystal. The parameters used were $\rho_{Na-O}$ = 0.30 Å and $\rho_{B-O}$ = 0.17 Å. The fraction of four-coordinated B atom, $N_4$, was calculated with various minimum interatomic $R_{B-O}$ distances. The compositional dependence of $N_4$ on various $R_{B-O}$ is shown in Figure 2. $N_4$ increases with increasing $Na_2O$ content and reaches a maximum value at around 40 mol % of $Na_2O$, and then it decreases. Furthermore, $N_4$ increases with increasing $R_{B-O}$ for each $Na_2O$ content indicating that the $BO_4$ units stabilize with an increase in the B−O distance. In the $^{11}$B NMR results,[20] $N_4$ increases along $X(1 - X)$, where $X$ = [$Na_2O$]. In Figure 2, $X(1 - X)$ is shown by the solid line. When $R_{B-O}$ was 1.17 Å, $N_4$ also increased along $X(1 - X)$. The calculated $N_4$ maximum is 0.41 at $Na_2O$ content of 40 mol %. This value is close to the maximum value of 0.39 at 40 mol % for $^{11}$B NMR. Accordingly, the optimized parameter set in the MD simulation of the $Na_2O-B_2O_3-SiO_2$ glasses was obtained from the results of $NaBO_2$ crystal and $Na_2O-B_2O_3$ glasses. The potential parameters are listed in Table 1.

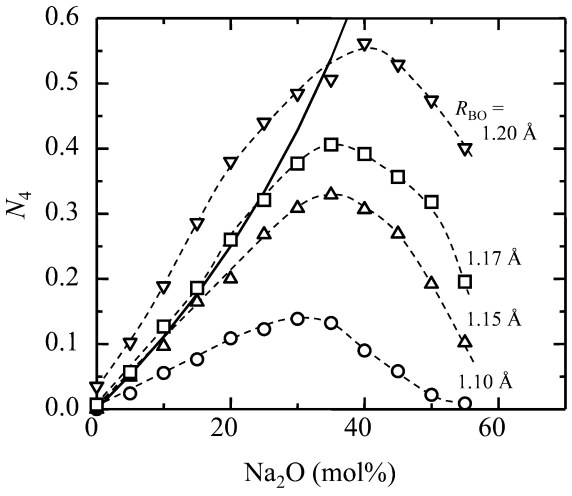


**Figure 2.** The fraction of four-coordinated B atoms, $N_4$, as a function of the $Na_2O$ content for various $R_{BO}$ values in the structural models of $Na_2O-B_2O_3$ glasses. The distances of $R_{BO}$ are 1.10 Å (circles), 1.15 Å (upward triangles), 1.17 Å (squares), and 1.20 Å (downward triangles). The solid line indicates $X(1-X)$, where $X$ is equal to the $Na_2O$ content.

**Table 1. Potential Parameters Used in the $Na_2O-B_2O_3-SiO_2$ System**

| M | $Z_M$ | $B_{M-O}(10^{-16}$ J) | $\rho_{M-O}$ (Å) |
|---|---|---|---|
| Na | +1.0 | 2.30 | 0.300 |
| B | +1.8 | 7.04 | 0.170 |
| Si | +2.4 | 19.6 | 0.174 |
| O | −1.20 ∼ −1.45 | 0.625 | 0.362 |

**(3). $Na_2O-B_2O_3-SiO_2$ glasses.** For all compositions, the oxygen coordination numbers of B atoms were 3 and 4. The coordination numbers of Si atoms ranged from 4.044 to 4.00 in 91 structural models.

We investigated the distribution of B−O and Si−O distances in the structural model with $R$ = 1 and $K$ = 2. The cutoff distances for the B−O and Si−O pairs were set at 2.0 and 2.5 Å, respectively. In 450 B atoms, there were 219 three-coordinated B ($^{[3]}$B) and 231 four-coordinated B ($^{[4]}$B). The average coordination number of the B atoms was 3.51. There were 450 Si atoms in which 442 were four-coordinated and 8 were five-coordinated. The average coordination number of Si atoms was 4.02.

The oxygen atoms coordinating with $^{[3]}$B, $^{[4]}$B, or Si are classified into four groups depending on the rest of the coordination, such as nonbridging oxygen (NBO), $^{[4]}$B (O−$^{[4]}$B), $^{[3]}$B (O−$^{[3]}$B), and Si (O−Si). Figure 3 shows the distributions of the distances between (a) $^{[3]}$B and NBO, (b) $^{[3]}$B and O−$^{[4]}$B, (c) $^{[3]}$B and O−$^{[3]}$B, and (d) $^{[3]}$B and O−Si. The distances of $^{[3]}$B−O pairs ranged from 1.3 Å to 1.45 Å. The average distance between $^{[3]}$B and NBO was 1.35 Å, and the average distances of $^{[3]}$B−O in $^{[3]}$B−O−$^{[4]}$B, $^{[3]}$B−O−$^{[3]}$B, and $^{[3]}$B−O−Si were 1.36, 1.37, and 1.38 Å, respectively. The $^{[3]}$B−O distances increased in this order. The distances of the $^{[4]}$B−O pairs ranged from 1.35 Å to 1.7 Å as shown in Figure 3e−h. The average distance between $^{[4]}$B and NBO was 1.48 Å, and the average distances of $^{[4]}$B−O in $^{[4]}$B−O−$^{[4]}$B, $^{[4]}$B−O−$^{[3]}$B, and $^{[4]}$B−O−Si were 1.46, 1.48, and 1.49 Å, respectively. The distances of $^{[4]}$B−O pairs increased in the same order of the $^{[3]}$B−O pairs except for the distance in the $^{[4]}$B−NBO pairs. The distances of $^{[4]}$B−O pairs were about 0.1 Å larger than those of $^{[3]}$B−O pairs. The distributions of the distance in the Si−O pairs are shown in Figure 3i−l. The average distance between Si and NBO was 1.58 Å, and the average distances of Si−O in Si−O−$^{[4]}$B, Si−O−$^{[3]}$B, and Si−O−Si were 1.58, 1.59, and 1.59 Å, respectively.

The distances between oxygen atoms and $^{[3]}$B, $^{[4]}$B, and Si in the structural models were consistent with the experimental values such as 1.37 Å for $^{[3]}$B−O,[20,21] 1.47 Å for $^{[4]}$B−O,[22] and 1.61 Å for Si−O.[23,24] The $^{[4]}$B−NBO bonds represent about 4% of the total $^{[4]}$B−O bonds. This value is considerably smaller than 9%, which is the proportion of the $^{[3]}$B−NBO bonds for total $^{[3]}$B−O bonds and also the proportion of the


dx.doi.org/10.1021/jp3038126 | J. Phys. Chem. B 2012, 116, 12325−12331

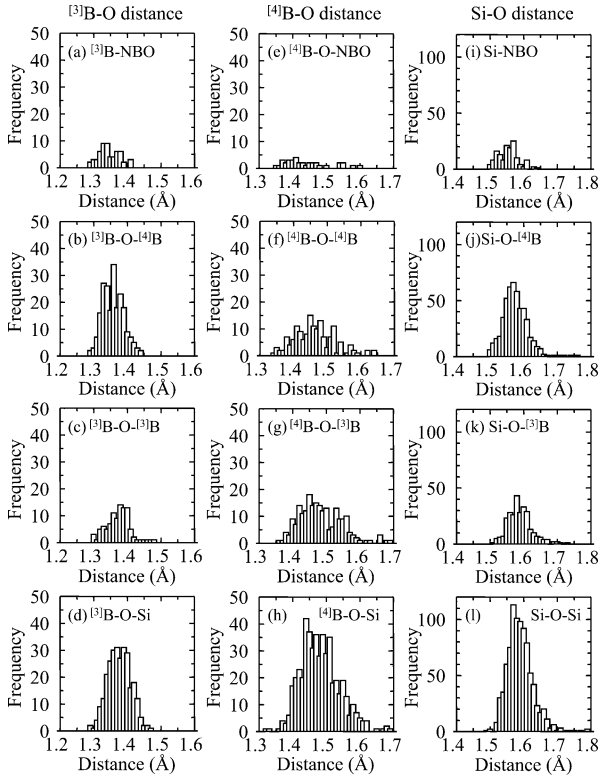


**Figure 3.** The distribution of pair distances in the structural models for $R$ = 1 and $K$ = 2. $^{[3]}$B−O distances at (a) $^{[3]}$B−NBO, (b) $^{[3]}$B−O(−$^{[4]}$B), (c) $^{[3]}$B−O(−$^{[3]}$B), and (d) $^{[3]}$B−O(−Si). $^{[4]}$B−O distances at (e) $^{[4]}$B−NBO, (f) $^{[4]}$B−O(−$^{[4]}$B), (g) $^{[4]}$B−O(−$^{[3]}$B), and (h) $^{[4]}$B−O(−Si). Si−O distances at (i) Si−NBO, (j) Si−O(−$^{[4]}$B), (k) Si−O(−$^{[3]}$B), and (l) Si−O(−Si).

Si−NBO bonds for total Si−O bonds. This indicates that NBOs are difficult to form in $BO_4$ units.

The fraction of $N_4$ in the structural model is compared with that of Dell's model on the basis of the $^{11}$B NMR results for various $K$ values. The $N_4$ value for each $K$ is shown in Figure 4a−g together with the calculated data using the equation in Dell's model. The maximum value of $N_4$, $N_{4,max}$, was 0.46 at $K$ = 0.5 in our structural model, which is slightly smaller than 0.53 in Dell's model as shown in Figure 4a. In Dell's model, $N_{4,max}$ increases with an increase of $K$ values. Since $N_{4,max}$ increased at a slower rate in our structural model, the difference between our structural model and Dell's model became larger with an increase of $K$ value as shown in Figure 4h. While $N_{4,max}$ reaches 0.88 at $K$ = 6 in Dell's model, that was 0.59 in our structural model. Therefore, it was found that the effect of adding $SiO_2$ was smaller than in Dell's model.

The compositional dependence of the NBO fraction is shown in Figure 5. The NBO fraction is the number of NBOs in the B−O and Si−O networks divided by the total number of oxygen atoms. The fraction of NBOs in the B−O and Si−O networks calculated with Dell's model is shown in Figure 5 as dotted and solid lines, respectively. The NBO fraction increased with an increase in $R$ for each value of $K$ and for our structural model as well as Dell's model, which is based on the results of $^{11}$B NMR. It is also found that the NBO fraction in the Si−O network increases with increasing $K$. Except in the low-$Na_2O$ region, there is relatively good agreement in the compositional dependence and NBO fraction values between the model and experimental data. Considering that NBOs are formed by Na

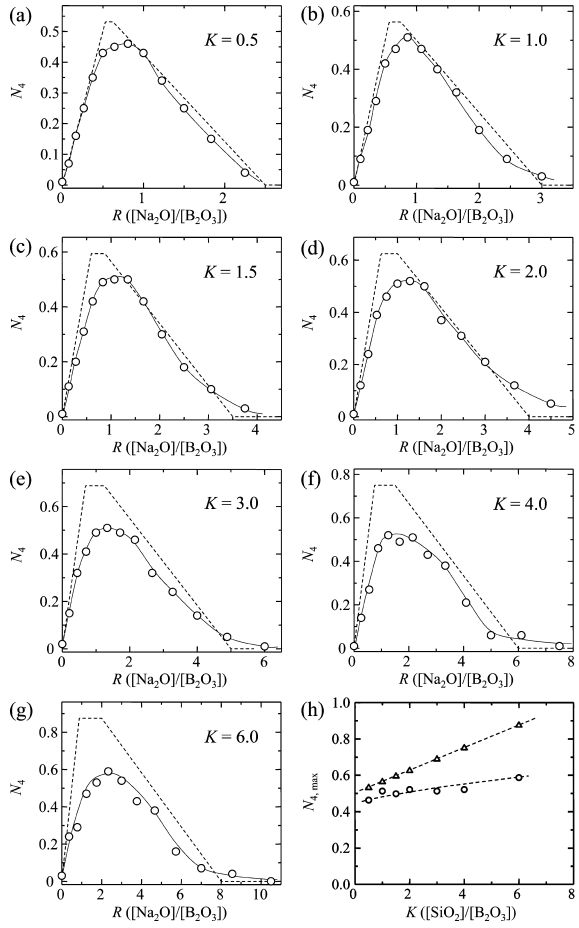


**Figure 4.** The $R$ (=[$Na_2O$]/[$B_2O_3$]) value dependence of the $N_4$ values in the structural models (circles) and in Dell's model (broken lines)[1] for (a) $K$ (=[$SiO_2$]/[$B_2O_3$]) = 0.5, (b) $K$ = 1.0, (c) $K$ = 1.5, (d) $K$ = 2.0, (e) $K$ = 3.0, (f) $K$ = 4.0, and (g) $K$ = 6.0. (h) The $K$ value dependence of the maximum value of $N_4$, $N_{4,max}$ in the structural models (circles) and in Dell's model (triangles). The dotted lines are guides to the eyes.

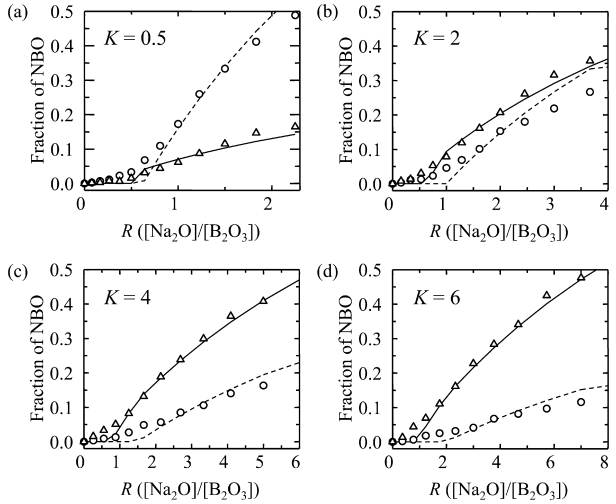


**Figure 5.** The fraction of NBOs in the B−O (circles) and Si−O (triangles) network. The series of glasses are (a) $K$ = 0.5, (b) $K$ = 2, (c) $K$ = 4, and (d) $K$ = 6. The solid and the dotted lines are calculated for the fraction of NBOs in the B−O and Si−O network, respectively, from the equation in Dell's model.[1]


dx.doi.org/10.1021/jp3038126 | J. Phys. Chem. B 2012, 116, 12325−12331

ions modifying the $BO_n$ or $SiO_n$ polyhedra, we can conclude that the fraction of Na ions can reproduce the experimental results over a wide compositional range.

However, at the low-$Na_2O$ region, there was remarkable difference between our structural model and Dell's model. In Dell's model, Na ions are assumed to be distributed only in the B−O network when they are initially introduced into the $B_2O_3$−$SiO_2$ glass. At that time, the coordination number of B atoms increases from 3 to 4, and NBOs are not formed. Furthermore, as the $Na_2O$ content increases, NBOs are formed in the Si−O network but not in the B−O network. NBOs in the B−O network are formed after introducing a relatively large number of Na ions in the B−O network after which $N_4$ reaches the maximum value. Subsequently, the Na ions are proportionally distributed between the B−O and Si−O networks. According to Dell's model, selective interaction between Na ions and the B−O network seems to exist at the beginning of $Na_2O$ addition. However, in our calculations, NBOs were formed in both B−O and Si−O networks even as $Na_2O$ was being added. This is a characteristic difference between our model and Dell's model.

Figure 6 shows the compositional dependence of oxygen species such as M′−O−M″ (M′, M″ = $^{[3]}$B, $^{[4]}$B, and Si) in our

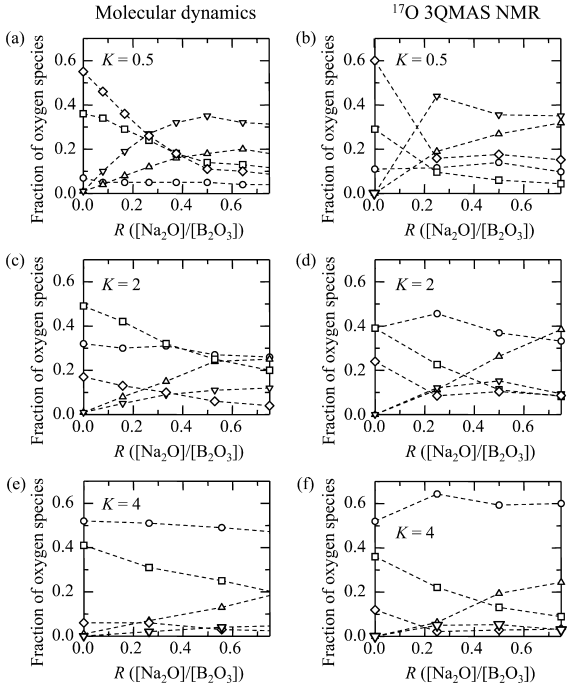


**Figure 6.** The fraction of oxygen species in the structural models and the $^{17}$O 3QMAS NMR spectra.[5] The series of glasses are (a, b) $K$ = 0.5, (c, d) $K$ = 2, and (e, f) $K$ = 4. The circles, upward triangles, squares, downward triangles, and diamonds represent Si−O−Si, Si−O−$^{[4]}$B, Si−O−$^{[3]}$B, $^{[4]}$B−O−$^{[3]}$B, and $^{[3]}$B−O−$^{[3]}$B, respectively. The dotted lines are simply visual guides.

model and the $^{17}$O 3QMAS NMR results[5] for various $K$ values. The fraction of Si−O−Si was almost constant in all graphs. The fractions of $^{[3]}$B−O−$^{[3]}$B and Si−O−$^{[3]}$B decreased with increasing $R$, whereas those of $^{[3]}$B−O−$^{[4]}$B and Si−O−$^{[4]}$B bonds increased. We found that our calculations could reproduce the $^{17}$O 3QMAS NMR results with 10% accuracy.

Figure 7 shows the compositional dependence of the distribution of $Q^n$ ($SiO_4$ tetrahedron with $n$ bridging oxygen)

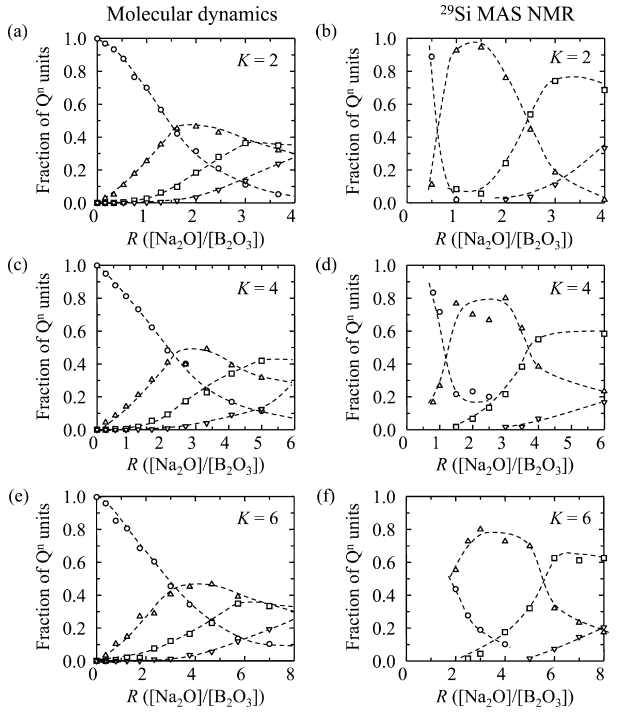


**Figure 7.** The fraction of each $Q^n$ unit in the structural model and the $^{29}$Si MAS NMR data.[9] The series of glasses are (a, b) $K$ = 2, (c, d) $K$ = 4, and (e, f) $K$ = 6. The circles, upward triangles, squares, and downward triangles represent $Q^4$, $Q^3$, $Q^2$, and $Q^1$, respectively. The dotted lines are simply visual guides.

in our structural model and the analysis of the $^{29}$Si MAS NMR results.[9] Although the distribution of each $Q^n$ extracted from the structural model exhibits almost the same compositional dependence as that in the experimental results, the fractions of each $Q^n$ unit were more widely distributed than those of the experimental results. The maxima of the fraction of $Q^3$ in our structural model were about 0.5 for all $K$ values, and the peak position shifted from $R$ = 2, 3, 4 for $K$ = 2, 4, 6, respectively. However, the maxima of the fractions of $Q^3$ in the experimental results were more than 0.8, and the peak positions were smaller than in the structural models. The observations revealed lower peak heights and broader distributions in the structural models than those in the experimental results.

## IV. DISCUSSION

In our structural model of $Na_2O$−$B_2O_3$−$SiO_2$ glasses, which is based on MD simulations using pair potentials, the average cation−oxygen distance in the various structural units are in reasonable agreement with that observed in the experiments. There are similarities and differences between the model data and the experimental results for the local structure around B, O, and Si. The similarities are as follows: (a) The $R$ value dependence of the $N_4$ values in the structural models corresponds to Dell's model and $N_{4,max}$ increases with the addition of $SiO_2$ (Figure 4); (b) NBOs are formed in both B−O and Si−O networks over a wide compositional range except in the low-$R$ region, and the proportion of NBOs formed in each network agrees with that in Dell's model as shown in Figure 5; (c) the distribution of the oxygen species can be reproduced within 10% of the $^{17}$O NMR results as shown in Figure 6; (d) the composition dependence of the distribution of the $Q^n$ species is qualitatively similar to that in the $^{29}$Si NMR


dx.doi.org/10.1021/jp3038126 | J. Phys. Chem. B 2012, 116, 12325−12331

results in Figure 7. These similarities are clear evidence that the quality of the structural information obtained from the computer simulation results has improved remarkably even if the potential used is a simple pair potential. In addition, these results indicate that the role of the interaction between the neighboring atoms is the most important parameter to capture the essence of amorphous materials.

The differences are as follows: (a) The values of $N_{4,max}$ are always smaller than those in Dell's model. The addition effect of $SiO_2$ on the $N_{4,max}$ value was smaller than that in Dell's model (Figure 4); (b) we could not observe selective interaction between Na ions and the B−O network in the low-$Na_2O$ or $R$ region (Figure 5); (c) the absolute values of the fraction $Q^n$ species were smaller than in $^{29}$Si MAS NMR data because of the relative broad distribution of the fraction (Figure 7). It is estimated that the differences are caused by the following three factors that are inevitable for our MD simulation. One is simplicity of our pair potential. The second one is the number of particles in the unit cell or the size of the unit cell. The periodicity of the unit cell with about 3000 particles is assumed in our simulation, which is an incredible difference from the real glass. The third one is the quenching rate which is at least 9 orders of magnitude larger than that of the real glass production. Therefore, the atomic arrangement obtained by MD simulation is that frozen at higher temperature. In other words, the atomic arrangement with higher entropy condition must be obtained. These three factors cannot be avoided, and it is difficult to divide each factor. Accordingly, it is not to say that MD simulation can produce an exact copy of the real glass structure with a high degree of accuracy. However, if one can make a correct assessment of the three factors, the origin of the differences between the simulated glass and the real glass can be explained.

The peak height decreasing because of the peak broadening in the distribution of the $Q^n$ in our model as shown in Figure 7 can be explained by using three equilibrium reactions.

$$\text{reaction 1:} \quad 2Q^3 \leftrightarrow Q^4 + Q^2 \tag{5}$$

$$\text{reaction 2:} \quad 2Q^2 \leftrightarrow Q^3 + Q^1 \tag{6}$$

$$\text{reaction 3:} \quad 2Q^1 \leftrightarrow Q^2 + Q^0 \tag{7}$$

The equilibrium constants, $K_1$, $K_2$, and $K_3$, for eqs 5−7, respectively, are given by

$$K_1 = \frac{[Q^4][Q^2]}{[Q^3]^2} \tag{8}$$

$$K_2 = \frac{[Q^3][Q^1]}{[Q^2]^2} \tag{9}$$

$$K_3 = \frac{[Q^2][Q^0]}{[Q^1]^2} \tag{10}$$

where $[Q^n]$ indicates the fraction of the $Q^n$ unit. The $[Q^n]$ units were counted in the structural models of $K$ = 2 and $R$ = 1.6−3.0, $K$ = 4 and $R$ = 2.69−5.0, and $K$ = 6 and $R$ = 3.77−7.0. There is almost no $K$ value dependence of $K_1$, $K_2$, and $K_3$. They were 0.33, 0.40, and 0.30 on average, respectively. The values of $K_1$ of $Na_2Si_2O_5$ glass ranged from 0.0045 for 400 °C to 0.01 for 603 °C reported by Maekawa and Yokokawa from $^{29}$Si NMR results.[25] Compared with the experimental values, the values of $K_1$, $K_2$, and $K_3$ in our structural models are quite large. From the obtained $K_n$ values, we can estimate the fictive temperature $T$ of the structural model by using these thermodynamic expressions

$$\Delta G = -RT \ln K_n \tag{11}$$

and

$$\Delta G = \Delta H - T\Delta S \tag{12}$$

where $\Delta G$, $R$, $\Delta H$, and $\Delta S$ are the free energy, the gas constant, the enthalpy, and the entropy, respectively. $\Delta H$ and $\Delta S$ for eq 5 of $Na_2Si_2O_5$ glass were evaluated as 27 kJ/mol and 7 J/K/mol, respectively.[25] Assuming that $\Delta H$ and $\Delta S$ can be applied to a wide temperature range, by using these values and $K_1$, the temperature $T$ of the structural model was calculated to be 1660 K. The high temperatures were also estimated for eqs 6 and 7 because $K_2$ and $K_3$ differ little from $K_1$. This means that the structural model should be in a higher temperature state although the MD simulation was finished at room temperature. It is reasonable to deduce that the higher temperature states are frozen even at room temperature because of the extremely higher quenching rate in the computer simulation than in the real experiment. As a result, it is suggested that the broadening in the distribution of the $Q^n$ was caused by the higher temperature state of the structural model.

The smaller $N_{4,max}$ than in Dell's model and the apparent absence of selective interaction between $Na_2O$ and $B_2O_3$ at the early stage of $Na_2O$ addition will be also explained by the higher temperature state because of the higher quenching rate. At the early stage of $Na_2O$ addition, Na ions can stay at various local structures in the state with higher entropy. This means that $Na_2O$ does not show strong selective interaction only with the B−O network. As a result, the NBOs are formed more easily both in the B−O and Si−O networks, and the values of $N_4$ decrease more than those in Dell's model. The inconsistency with Dell's model in the $K$ value dependence of the $N_4$ values might be due to the simplicity of our potentials.

Although there are unavoidable limitations in the molecular dynamics simulation, this technique can provide the atomic arrangement and the coordination number of each ion in a model glass as in a real glass even if the potential is a two-body system. From the obtained local structure, we can more precisely predict the physical properties of a glass. Three-dimensional structures without any physical inconsistency can be obtained. In the three-dimensional structure, not only the nearest neighbor but also the second nearest neighbor can be shown. Therefore, we believe the molecular dynamics technique using pair potentials is a suitable method to develop structural models for estimating and analyzing the relation between physical properties and structure.

## V. CONCLUSION

A structural model of sodium borosilicate glasses was prepared by using a molecular dynamics approach using pair potentials. The average coordination number of B and Si atoms and the average distance between cations and oxygen in various structural units are in good agreement with experimental results. We found similarities and differences in the local structure between model and experimental data. The similarities support the usefulness of the molecular dynamics simulations in modeling the glass structure even if pair potentials are used. The factors responsible for these differences were discussed with respect to the equilibrium reactions between the cation−oxygen polyhedra at a higher temperature.

It was shown that the differences were caused by the extremely higher quenching rate than in the real glasses as well as by the simplicity of our pair potential and the smaller size of the unit cell. These results confirm that even a simple MD technique that uses pair potentials is adequate in capturing the essence of amorphous materials if one can make a correct assessment of the three factors.

## AUTHOR INFORMATION

### Corresponding Author

*Tel.: +81-3-545-6315; fax: +81-3-5452-6316; e-mail: masuno@iis.u-tokyo.ac.jp.

### Notes

The authors declare no competing financial interest.

## ACKNOWLEDGMENTS

This work was performed as a project for Research and Development to Promote the Creation and Utilization of Intellectual Infrastructures of New Energy and Industrial Technology Development Organization in Japan (NEDO) from 2005 to 2007.

## REFERENCES

(1) Dell, W. J.; Bray, P. J.; Xiao, S. Z. *J. Non-Cryst. Solids* **1983**, *58*, 1−16.
(2) Zhong, J.; Wu, Z.; Liu, M. L.; Bray, P. J. *J. Non-Cryst. Solids* **1988**, *107*, 81−87.
(3) Wang, S.; Stebbins, J. F. *J. Am. Ceram. Soc.* **1999**, *82* (6), 1519−1528.
(4) Du, L.-S.; Stebbins, J. F. *J. Non-Cryst. Solids* **2003**, *315*, 239−255.
(5) Du, L.-S.; Stebbins, J. F. *J. Phys. Chem. B* **2003**, *107*, 10063−10076.
(6) Ogawa, H.; Sugiyama, K.; Waseda, Y.; Shiraishi, Y. *J. Non-Cryst. Solids* **1992**, *143*, 201−206.
(7) Delaye, J. -M.; Cormier, L.; Ghaleb, D.; Calas, G. *J. Non-Cryst. Solids* **2001**, *293*−*295*, 290−296.
(8) Martin, S. W.; Mackenzie, J. W.; Bhatnagar, A.; Bhowmik, S.; Feller, S. A.; Royle, M. L. *Phys. Chem. Glasses* **1995**, *36* (2), 82−88.
(9) Bhasin, G.; Bhatnagar, A.; Bhowmik, S.; Stehle, C.; Affatigato, M.; Feller, S.; Mackenzie, J.; Martin, S. *Phys. Chem. Glasses* **1998**, *39* (5), 269−274.
(10) Miura, Y.; Kusano, H.; Nanba, T.; Matsumoto, S. *J. Non-Cryst. Solids* **2001**, *290*, 1−14.
(11) Manara, D.; Grandjean, A.; Neuville, D. R. *J. Non-Cryst. Solids* **2009**, *355*, 2528−2531.
(12) Soules, T. F.; Varshneya, A. K. *J. Am. Ceram. Soc.* **1981**, *64* (3), 145−150.
(13) Kieu, L.-H.; Delaye, J.-M.; Cormier, L.; Stolz, C. *J. Non-Cryst. Solids* **2011**, *357*, 3313−3321.
(14) Marezio, M.; Plettinger, H. A.; Zachariasen, W. H. *Acta Crystallogr.* **1963**, *16*, 594−595.
(15) Berens, P. H.; White, S. R.; Wilson, K. R. *J. Chem. Phys.* **1981**, *75*, 515−529.
(16) Budhwani, K.; Feller, S. *Phys. Chem. Glasses* **1995**, *36* (4), 183−190.
(17) Inoue, H.; Saito, Y. *Proceedings of the 2007 ACerS Glass & Optical Materials Division Meeting & 18th University Conference on Glass*; Wiley-VCH Verlag GmbH & Co. KGaA, S1-5-1−S1-5-5.
(18) Chryssikos, G. D.; Kapoutsis, J. A.; Patsis, A. P.; Kamitsos, E. I. *Spectrochim. Acta, Part A* **1991**, *47* (8), 1117−1126.
(19) Wu, K.; Lee, S.-Y. *J. Phys. Chem. A* **1997**, *101*, 937−940.
(20) Zhong, J.; Bray, P. J. *J. Non-Cryst. Solids* **1989**, *111*, 67−76.
(21) Mozzi, R. L.; Warren, B. E. *J. Appl. Crystallogr.* **1970**, *3*, 251.
(22) Swenson, J.; Börjesson, L.; Howells, W. S. *Phys. Rev. B* **1995**, *52* (13), 9310−9319.
(23) Mozzi, R. L.; Warren, B. E. *J. Appl. Crystallogr.* **1969**, *2*, 164.
(24) Misawa, M.; Price, D. L.; Suzuki, K. *J. Non-Cryst. Solids* **1980**, *37*, 85−97.
(25) Maekawa, H.; Yokokawa, T. *Geochim. Cosmochim. Acta* **1997**, *61*, 2569−2575.